of analysis accounting for the total heat transfer from the surface due to sliding bubbles must therefore include both mechanisms.

REFERENCES

1. K. Cornwell, The influence of bubbly flow on boiling from a tube in a bundle, *Int. J. Heat Mass Transfer* **33**, 2579–2584 (1990).
2. K. Cornwell, S. D. Houston and A. J. Addlesee, Sliding bubble heat transfer on a tube under heating and cooling conditions. In *Pool and External Flow Boiling* (Edited by V. K. Dhir and A. E. Bergles), pp. 49–53. New York ASME (1992).
3. Y. Yan and D. B. R. Kenning, Heat transfer near sliding vapour bubbles in boiling, *Tenth International Heat Transfer Conference, Brighton, U.K., Heat Transfer* 1994, Vol. 5, pp. 195–200 (1994).

Pergamon

Int. J. Heat Mass Transfer. Vol. 39, No. 1, pp. 214–218, 1996

0017-9310/96 $9.50+0.00

0017–9310(95)00074–7

Application of the diffuse approximation for solving fluid flow and heat transfer problems

H. SADAT and C. PRAX

Laboratoire d'Etudes Thermiques, URA CNRS 1403 ENSMA, Site du futuroscope, 86960 Futuroscope Cedex, France

(*Received* 7 *June* 1994 *and in final form* 15 *February* 1995)

1. INTRODUCTION

In the numerical simulation of fluid flow problems in regions with arbitrary shaped boundaries, finite-element methods (FEM) [1–3] and control-volume based finite-element methods [4–6] are generally used. For problems in which the position of large solution gradients is known *a priori*, such as those involving boundary layers, localized grid refinement can be used in these regions. There are several problems, however, where the position of steep gradients is not always known *a priori*. This is the case of compressible flows for example. Adaptive procedures for finite-element meshes are then necessary. Mesh generation and mesh enrichment are the most popular methods [7]. These techniques are time consuming and there is currently a great deal of research being done in this field [8].

The diffuse approximation method (DAM) is a new method for finding estimates of a scalar field φ and its derivatives [9, 10]. The starting point is to estimate the Taylor expansion of φ at a chosen point $M_i(x_i, y_i)$ by a weighted least squares method which uses only the values of φ at the nearest points $M_j(x_j, y_j)$. The main advantage of this method is that it only requires sets of discretization nodes and no geometric finite elements. These nodes could be generated by several techniques such as random shooting methods or octree-based methods. In any case it is much easier to generate nodal points than to build finite-element meshes. This method has been successfully used for steady-state diffusion problems [10, 11]. It has been shown that the DAM is much better than the FEM for the computation of gradients [9, 10]. Moreover it ensures uniform convergence of the successive derivate estimates when the sampling point density increases [10]. Application of the DAM to the post-treatment of electromagnetic field computations has been reported [12].

To date no attempt appears to have been made to apply the diffuse approximation in the field of computational fluid dynamics. Thus the main objective of this work is to demonstrate that this new method can be used to solve fluid flow and heat transfer problems with sufficient complexities that a fair test of the formulation can be made.

In the following sections, the formulation of the diffuse approximation is presented and applied to three example problems.

2. THE DIFFUSE APPROXIMATION

For a scalar field $\varphi(x, y)$ defined in a two-dimensional domain, let us pick a set of N points $M_i(x_i, y_i)$ in the vicinity of a chosen point $M(x, y)$. The diffuse approximation provides estimates of φ and its derivates at M from the nodal values φ_i. The basic idea is to estimate the Taylor expansion of φ at M by a weighted least squares method which uses only the values of φ at the nearest points M_i. By truncating the series at order k, one obtains the corresponding estimates of the derivatives at order k.

Therefore, as far as we are concerned by second-order partial differential equations, a second-order expansion is sufficient. Let us then estimate the second-order Taylor expansion of φ_i at M as:

$$\varphi_i = \sum_{j=0}^{5} P_{ij} \cdot \alpha_j \tag{1}$$

where

$$[P_{ij}] = [1, (x_i - x), (y_i - y), (x_i - x)^2, (x_i - x) \cdot (y_i - y), (y_i - y)^2]$$

and

NOMENCLATURE

$\mathscr{D}$	continuum domain	v^*	dimensionless vertical velocity $v^* = vL/\nu$
I	functional	T	temperature.
p	column vector of monomials		
p^T	p-transpose		
M	current point		
Nu	Nusselt number		
Pr	Prandtl number	Greek symbols	
R_i	inner cylinder radius	α	vector of estimated derivate
R_o	outer cylinder radius	γ	normal angle
Ra	Rayleigh number	ν	kinematic viscosity
Re	Reynolds number	φ	scalar field
x, y	Cartesian coordinates	ψ	stream-function
u, v	velocity components in the x and y directions	ω	vorticity
		$\omega_i(M,M_i)$	weight-function.

$$[\alpha]^T = [\alpha_0, \alpha_1, \alpha_2, \alpha_3, \alpha_4, \alpha_5].$$

The α_j coefficients are the estimates of φ and its successive derivatives up to order 2 at M. These coefficients are now determined by minimizing the quantity:

$$I(\alpha) = \sum_{i=1}^{N} \omega_i(M, M_i) \cdot \left[\varphi_i - \sum_{j=0}^{5} P_{ij} \cdot \alpha_j \right]^2 \quad (2)$$

where $\omega_i(M, M_i)$ is a weighting function which peaks at M and decays rapidly. Thus only the nearest points to M are involved in (2). By writing the six conditions:

$$\frac{\partial I}{\partial \alpha_j} = 0 \quad (3)$$

one gets the following (6×6) linear system:

$$\sum_{i=1}^{N} \omega_i(M, M_i) P_{ij} \cdot \left(\sum_{j=0}^{5} P_{ij} \alpha_j \right) = \sum_{i=1}^{N} \omega_i(M, M_i) P_{ij} \varphi_i \quad (4)$$

where $j = 0.5$.

Once the system (4) has been solved and the α_j have been determined, one finally obtains the desired approximate values at M:

$$\varphi(x, y) = \alpha_0 \quad \frac{\partial \varphi}{\partial x} = \alpha_1 \quad \frac{\partial \varphi}{\partial x} = \alpha_2$$

$$\frac{\partial^2 \varphi}{\partial x^2} = 2 \cdot \alpha_3 \quad \frac{\partial^2 \varphi}{\partial x \partial y} = \alpha_4 \quad \frac{\partial^2 \varphi}{\partial y^2} = 2\alpha_5. \quad (5)$$

3. APPLICATION TO FLUID FLOW PROBLEMS

Suppose that the governing equation for the scalar field φ is the convection–diffusion equation:

$$\frac{\partial u\varphi}{\partial x} + \frac{\partial v\varphi}{\partial y} = \Gamma \Delta \varphi + S. \quad (6)$$

By assigning different meanings of Γ and S one can recover different equations of fluid flow and heat transfer problems.

In order to solve equation (6), we first replace the continuum domain $\mathscr{D}$ by a pattern of discrete points within $\mathscr{D}$. The chosen weighting function is then used to select a number of points around each isolated point where the diffuse approximation of equation (6) is finally written. This leads to a linear system whose unknowns are the nodal values φ_i. The resulting matrix is sparse and without any particular structure.

In this work, the vorticity–stream-function formulation of the Navier–Stokes equations is used. Thus, the question of how pressure and velocity are coupled does not arise. The transport equations for vorticity ω, stream-function ψ and temperature T are solved sequentially, first for ψ, then for T and finally for ω. Relaxations factors are used for each variable.

4. BOUNDARY CONDITIONS AND CONVERGENCE CRITERIA

Dirichlet-type boundary conditions are introduced directly in the matrix system while Neumann boundary conditions are introduced via the α coefficients. The normal derivative at a boundary node is:

$$\frac{\partial \varphi}{\partial n} = \cos(\gamma) \cdot \frac{\partial \varphi}{\partial x} + \sin(\gamma) \cdot \frac{\partial \varphi}{\partial y}$$

where γ is the normal angle. Using equation (7), this can be written as follows:

$$\frac{\partial \varphi}{\partial n} = \cos(\gamma) \cdot \alpha_1 + \sin(\gamma) \cdot \alpha_2.$$

Now α_1 and α_2 are expressed as functions of nodal values of φ at the neighbouring nodes by inverting system (4). This leads to an equation relating these nodal values to the value of φ at the boundary node.

Unlike the boundary conditions for the stream-function and temperature, which are invariable and specified, the vorticity values at the boundary are not known *a priori* and are calculated in terms of the neighbouring stream-function values. Different formulations can be employed for this purpose [13]. In this work, the method used by Kettleborough *et al.* [14] is followed.

The convergence criteria used for the numerical calculations includes the relative changes between consecutive iterations:

$$\left| \frac{\psi_{new} - \psi_{old}}{\psi_{new}} \right|_{max} \leqslant 10^{-3};$$

$$\left| \frac{\omega_{new} - \omega_{old}}{\omega_{new}} \right|_{max} \leqslant 10^{-3}; \quad \left| \frac{T_{new} - T_{old}}{T_{new}} \right|_{max} \leqslant 10^{-3}$$

where ψ, ω, T are the stream-function, the vorticity and the temperature respectively.

5. WEIGHTING FUNCTIONS

When applying the DAM, one important choice is the weighting function. These functions can be chosen in many ways. Triangular, Hanning and Gaussian functions are easy

to implement and have proven to work well. Of course additional numerical studies need to be done before the advantages and disadvantages of these different windows can be known.

The results presented in this study have been obtained by using the following Gaussian window:

$$\omega_1(M, M_i) = \exp[-(r/\lambda)^2]$$

where r is the distance between M and M_i. The choice of λ gives us the practical window aperture as $\lambda/2\ln(10)$. In this work the window aperture has been chosen large enough to overlap at least 6 nodal points around the computational point.

6. NUMERICAL EXAMPLES

In this section the present method is applied to three overworked problems for which benchmark solutions are available.

6.1. *Driven cavity*

We first examine the case of the driven cavity. The flow was computed at Reynolds number based on the wall velocity and the cavity height ranging from 100 to 1500. Results were obtained on two uniformly spaced grids of 10×10 and 20×20 grid points. A relaxation factor of 0.2 was used for stream-function and vorticity. Table 1 gives the values of the maximum stream-function in the central vortex. The computed u-velocity profiles at the vertical midsection of the cavity at Reynolds number 400 and 1000 are presented in Figs. 1 and 2 For comparison, the results of Ghia *et al.* [15] have been included. From these figures, it can be seen that the proposed method produces good results even with relatively coarse grids, and it has the expected asymptotic behaviour as the grid is refined.

6.2. *Natural convection in a square cavity*

We now discuss the case of natural convection in a square cavity. In the present work, numerical results using the diffuse approximation have been obtained for Rayleigh numbers between 10^3 and 10^5 on the two uniform grids presented before. Table 2 compares the calculated Nusselt numbers which have been used as a basis for comparison with those obtained by De Vahl Davis [16]. The results are in good agreement with the benchmark solution, especially for the lower Rayleigh numbers. At higher Rayleigh numbers more points are needed near the walls for an accurate evaluation of the temperature gradient. Figure 3 shows variation of vertical velocity ($\mathbf{v}^* = vL/\nu$) along the horizontal midplane ($y/L = 0.5$) for a Rayleigh number of 5×10^4. The abbreviations DAM and CVFEM stand for the diffuse approximation method and the control-volume finite-element method that we have used for comparison.

As is evident from this figure, the diffuse approximation method produces results as good as those from the well known control-volume-based finite-element method [4–6].

6.3. *Natural convection in an annular space*

It remains to be demonstrated that the method can be used in arbitrary shaped geometries. To this end, we consider

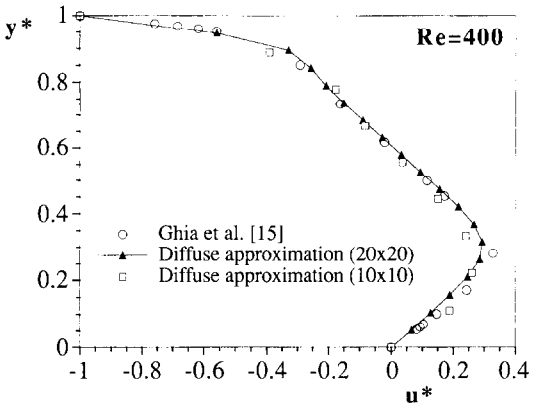

Fig. 1. Comparisons of u-velocity along a vertical line through the geometric center of the driven cavity with a Reynolds number of 400.

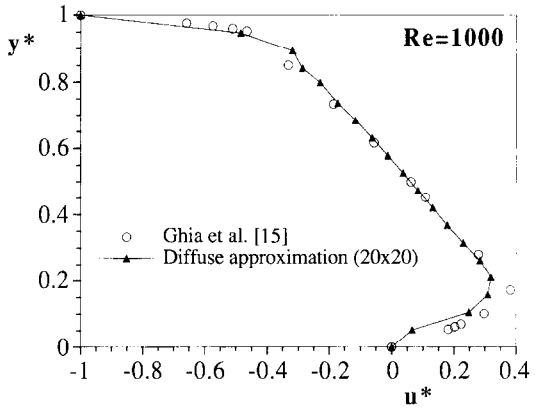

Fig. 2. Comparisons of u-velocity along a vertical line through the geometric center of the driven cavity with a Reynolds number of 1000.

Table 2. Results for the global Nusselt number in the natural square cavity

Rayleigh number	10^3	10^4	10^5
Reference [16] (41×41)	1.116	2.234	4.487
This work (20×20)	1.117	2.301	4.533

Table 1. Results for the maximum value of ψ in the driven cavity

Reynolds number	100	400	1000	1500
Reference [15] (129×129)	0.103 423	0.113 9423	0.117 929	0.120 377
This work (20×20)	0.102 44	0.107 57	0.107 35	0.106 64
This work (10×10)	0.097 9	0.102 2	—	—

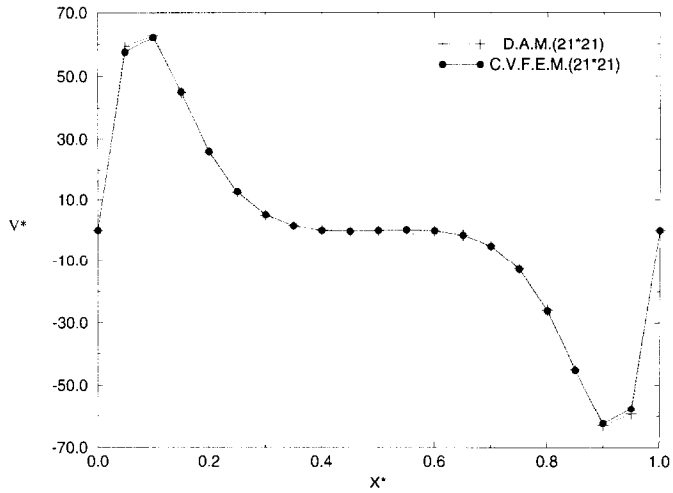

Fig. 3. Vertical velocity profile along the horizontal midplane of the cavity.

briefly here the case of natural convection in the two-dimensional annular space shown in Fig. 4. In this case, a triangular finite-element mesh was generated and the vertices of the triangular elements were used as calculation points. The mesh consisted of 506 grid points (16 points in the radial direction 20 points in the inner angular direction and 40 points in the outer angular direction). The calculations were carried out for an annulus with a radius ratio of 2.6 and using air ($Pr = 0.7$) as the working fluid. Here again, Nusselt numbers have been calculated. They are reported in Table 3 together with the results of reference [17]. As in the previous examples, we again find that the diffuse approximation method gives accurate results.

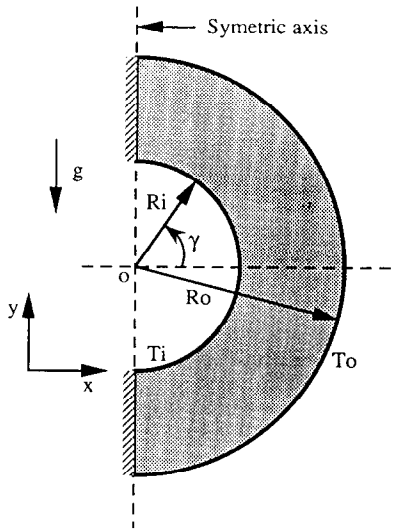

Fig. 4. Annular space.

7. CONCLUSION

In the present work, the diffuse approximation method is presented and applied to the solution of fluid flow and heat transfer problems. This method provides solutions comparable in accuracy to standard numerical methods. Comparative results of test cases show good agreement and validate the applicability of the method. However, the work which has been reported is still exploratory and further effort is needed to fully explore the limitations of the formulation.

REFERENCES

1. C. R. S. Swaminathan and V. R. Voller, Streamline upwind scheme for control-volume finite elements, Part I. Formulations, *Numer. Heat Transfer, Part B* **22,** 95–107 (1992).
2. S. Ramadhyani and S. V. Patankar, Solution of the convection-diffusion equation by a finite-element method using quadrilateral elements, *Numer. Heat Transfer* **8,** 595–612 (1985).
3. G. E. Schneider, Elliptic systems, finite-element method I. In *Handbook of Numerical Heat Transfer* (Edited by W. J. Minkowycz, E. M. Sparrow, G. E. Schneider, R. H. Pletcher), Chap. 10, pp. 379–420. Wiley, New York (1988).
4. B. R. Baliga and S. V. Patankar, A new finite-element formulation for convection–diffusion problems. *Numer. Heat Transfer* **3,** 393–409 (1980).

Table 3. Results for the global Nusselt number in the inner and outer cylinder of the annular space

Rayleigh number	Inner cylinder [17]	Inner cylinder [this work]	Outer cylinder [17]	Outer cylinder [this work]
10^3	1.081	1.089	1.084	1.091
3×10^3	1.404	1.405	1.402	1.412
10^4	2.010	1.993	2.005	2.003
2×10^4	2.405	2.421	2.394	2.436

5. B. R. Baliga and S. V. Patankar, A control volume finite-element method for two-dimensional fluid flow and heat transfer, *Numer. Heat Transfer* **6**, 245–261 (1983).
6. C. Prakash and S. V. Patankar, A control volume-based finite-element method for solving the Navier–Stokes equations using equal-order velocity-pressure interpolation, *Numer. Heat Transfer* **8**, 259–280 (1985).
7. R. Ramakrishnan, K. S. Bey and E. A. Thornton, Adaptative quadrilateral and triangular finite-element scheme for compressible flows. *AIAA J.* **28**, 51–59 (1990).
8. R. A. Shapiro and E. Murman, Adaptive finite element methods for the Euler equations. AIAA Paper 88-0034 (Jan. 1988).
9. B. Nayroles, G. Touzot and P. Villon, The diffuse elements method, *C. R. Acad. Sci. Paris, Série II*, **313**, 133–138 (1991).
10. B. Nayroles, G. Touzot and P. Villon, The diffuse approximation, *C. R. Acad. Sci. Paris, Série II*, **313**, 293–296 (1991).
11. B. Nayroles, G. Touzot and P. Villon, Generalizing the finite element method. Diffuse approximation and diffuse elements, *Comput. Mech.* **10**, 307–318 (1992).
12. Y. Marechal, J. L. Coulomb, G. Meunier and G. Touzot, Use of the diffuse element method for electromagnetic field computation., *IEEE Trans. Mag.* **29**, (1993).
13. M. S. Krakov, Control volume finite-element method for Navier–Stokes equations in vortex-streamfunction formulation, *Numer. Heat Transfer, Part B* **21**, 125–145 (1992).
14. C. F. Kettlebourough, S. R. Hussain and C. Prakash, Solution of fluid flow problems with the vorticity-streamfunction formulation and the control-volume-based finite-element method. *Numer. Heat Transfer, Part B* **16**, 31–58 (1989).
15. U. Ghia, K. N. Ghia and C. T. Shin, High-resolutions for incompressible flow using the Navier–Stokes equations and a multigrid method, *J. Comput. Phys.* **48**, 387 411 (1982).
16. G. De Vahl Davis, University of New South Wales, Kensington 2033, Australia : natural convection of air in a square cavity : a bench mark numerical solution, *Int. J. Numer. Methods Fluids* **3**, 249–264 (1983).
17. T. H. Kuehn and R. J. Goldstein, An experimental and theorical study of natural convection in the annulus between horizontal concentric cylinders, *J. Fluid Mech.* **74**, part 4, 695–719 (1976).

Pergamon

Int. J. Heat Mass Transfer. Vol. 39, No. 1, pp. 218–220, 1996

0017-9310/96 $9.50 + 0.00

0017-9310(95)00090-9

Remarks upon the contribution of J. Stefan to the understanding of diffusion processes

J. MITROVIC

Institut für Technische Thermodynamik und Thermische Verfahrenstechnik, Universität Stuttgart, 70550 Stuttgart, Germany

(*Received* 22 *November* 1994)

INTRODUCTION

Following his molecular theory of gases, Maxwell [1] arrived in 1866 at an equation describing the movement of a component by diffusion caused by a concentration gradient in a mixture. Concerning this publication by Maxwell, Stefan [2] noted: "Das Studium der Maxwell'schen Abhandlung ist nicht leicht".† He felt prompted to give an illustrative explanation of the diffusion processes in the light of hydrodynamic laws. Stefan clearly recognized that diffusion can give rise to a convective movement in the mixture. He also derived an equation for the calculation of the total transport rate of a component caused by diffusion in a mixture with a concentration gradient.

Onsager and Fuoss [3] seem to be the first who clearly distinguished between the different transport mechanisms and suggested a calculation of the total transport of a component as a sum of diffusion and convection movement. At about the same time as Onsager and Fuoss, Kuusinen [4] discussed the concept of diffusion to some extent. According to his opinion, the diffusion process is seen as a movement of a component relative to the average velocity of the mixture. Disregarding the clear formulation of the diffusion process, new elements in a physical sense compared with Stefan's view of diffusion are scarce in Kuusinen's publication. Later on, the same questions were considered by Darken [5] and Hartley and Crank [6], who gave a precise explanation of the diffusion process and of the diffusion-caused convection in mixtures using markers in diffusion space and coordinate transformation.

According to Kuusinen [4], Darken [5] and Hartley and Crank [6], the total flow rate $\dot{n}_j$ of a component j in a binary mixture with a concentration gradient should be calculated by

$$\dot{n}_j = J_j + Y_j\dot{n}. \tag{1}$$

In this equation, Y_j is the mole fraction of the component j, $\dot{n}$ is the sum of all flow rates in the diffusion space and J_j is the flow rate by pure diffusion, see Fig. 1.

For a binary mixture consisting of the components j and k, the total flow rate $\dot{n}$ of the mixture is given by

† 'Maxwell's considerations are not simple.'